Di Dato, M., D'Angelo, C., Casasso, A., Zarlenga, A. (2022):
The impact of porous medium heterogeneity on the thermal feedback of open-loop shallow geothermal systems
J. Hydrol. **604** , art. 127205

Highlights

The impact of porous medium heterogeneity on the thermal feedback of open-loop shallow geothermal systems

Mariaines Di Dato, Claudia D'Angelo, Alessando Casasso, Antonio Zarlenga

- Heterogeneity has a relevant impact on geothermal system efficiency.
- Heterogeneity of hydraulic conductivity affects the transient of thermal feedback.
- Heterogeneity and dispersivity do not affect long-term behaviour of well doublets.
- Uncertainty increases with medium heterogeneity in non-ergodic conditions.

The impact of porous medium heterogeneity on the thermal feedback of open-loop shallow geothermal systems

Mariaines Di Dato[a,*], Claudia D'Angelo[b], Alessando Casasso[c], Antonio Zarlenga[b]

[a]*Department of Computational Hydrosystems, Helmholtz Centre for Environmental Research - UFZ, Permoserstraße 15, Leipzig, 04318, Germany*

[b]*Department of Engineering, Roma Tre University, Via Vito Volterra 62, Rome, 00146, Italy*

[c]*Department of Environment, Land and Infrastructure Engineering (DIATI), Politecnico di Torino, Corso Duca degli Abruzzi 24, Torino, 10129, Italy*

Abstract

Groundwater has been increasingly used to provide low-carbon heating and cooling of buildings with open-loop shallow geothermal systems. Water is generally reinjected into the same aquifer after the heat exchange in order to avoid the aquifer depletion. However, this can result in the return of part of the injected water to the production well(s), causing a gradual thermal alteration known as thermal feedback. Thermal feedback is a major design issue of open-loop shallow systems but, so far, it has been mainly addressed neglecting the heterogeneity of the aquifer properties. This study investigates the impact of aquifer heterogeneity on two main metrics that characterize thermal feedback: thermal breakthrough time (i.e., the first arrival time of the thermal plume) and recirculating ratio (i.e., the fraction of water coming back to production well). A stochastic approach was adopted performing a large number of numerical simulations that cover a wide range of possible scenarios. Results highlight that conductivity heterogeneity plays a major influence on the temperature evolution at the production well. The breakthrough time alone might lead to misleading evaluations of the system efficiency, given that a few particles can reach the production well by traveling in the highly-conductive layers. Conversely, both the heterogeneity and the thermal dispersivity have a negligible impact on the recirculating ratio, which quantifies the long-term evolution of thermal feedback. As a consequence, the available approaches based on advection-only and homogeneous medium are a robust tool to predict the long-term behaviour of shallow open-loop geothermal systems.

Keywords: Geothermal systems, Thermal feedback, Thermal breakthrough time, Stochastic

*Corresponding author

Email address: mariaines.di-dato@ufz.de (Mariaines Di Dato)

approach, Aquifer heterogeneity

1. Introduction

The use of shallow geothermal energy for heating and cooling of buildings has become popular thanks to the low operational costs and the low carbon intensity (Casasso and Sethi, 2019; Bayer et al., 2019; Lund and Toth, 2020; Tissen et al., 2021; Bartolini et al., 2020). The heat in the subsurface can be exploited by shallow geothermal systems in two ways: through the circulation of a heat carrier fluid into a closed pipe loop (closed-loop systems) or by exchanging heat with groundwater (open-loop systems). Generally speaking, closed-loop systems are installed in the absence of an exploitable aquifer or, for small-power installations (e.g., below 100 kW), to avoid the maintenance issues typical of wells. Open-loop systems are more popular for large-scale installations up to a few MW thanks to their higher efficiency and the economies of scale (Tsagarakis et al., 2020). Large flow rates in the order of tens or even hundreds of L/s are abstracted to provide such a large thermal power and, for this reason, water is generally reinjected into the same aquifer to avoid its depletion and depressurization (Horne, 1985; Banks, 2012).

However, reinjection raises a few possible issues, among which the return to the production well(s) of a share of the reinjected water (Milnes and Perrochet, 2013). Since the temperature of reinjected water is different from the background value of the aquifer (i.e., colder when the plant operates in heating mode, and hotter when it operates in cooling mode), the abstracted water progressively decreases or increases its temperature. Such a process occurs at the production well only under certain hydraulic conditions, which are seldomly avoidable in densely-populated urban areas (Clyde and Madabhushi, 1983; Kong et al., 2017). The gradual thermal alteration of abstracted water is defined *thermal feedback* or *thermal recycling* according to the operating parameter imposed, that is, respectively, the reinjection temperature or the temperature difference between reinjected and abstracted water (Milnes and Perrochet, 2013). This study adopts constant reinjection temperatures and therefore focuses on the issues related to thermal feedback, which might gradually compromise the efficiency of the geothermal plant even to its failure (Banks, 2009). In order to prevent this, the temperature of reinjected water has a minimum and a maximum limit. The minimum temperature allowed is, theoretically, the water icing (0°C); however, a safety margin must be imposed on this value. The maximum temperature allowed depends on technical constraints, such as the operating limits imposed by the heat pump manufacturer or the HVAC (Heating, Ventilation, and Air Conditioning) designer and on legislative constraints. Indeed, reinjection of warm water has several potentially negative impacts on groundwater ecosystems and on groundwater quality (Casasso and Sethi, 2019), as well as on neighbouring and downstream shallow geothermal installations (Epting et al., 2017; Barla et al., 2018; Pophillat et al., 2020).

Thermal feedback is therefore a major design issue for open-loop shallow geothermal systems. So far, the literature addressed this issue mainly considering a homogeneous porous medium. Early publications (Gringarten and Sauty, 1975; Lippmann and Tsang, 1980) and more recent works (Luo and Kitanidis, 2004; Milnes and Perrochet, 2013; Kong et al., 2017) provided the mathematical framework to address thermal feedback under the following assumptions: i) homogeneous porous medium, ii) constant operating conditions (flow rate, temperature difference), and iii) a well doublet aligned with groundwater flow. Recently, Casasso and Sethi (2015) developed a MATLAB code to assess thermal feedback with arbitrary well doublet alignments and derived an empirical formula to estimate the time trend of well temperatures for wells aligned with groundwater flow.

However, solutions based on homogeneous conductivity and effective macrodispersion coefficients are not able to grasp the effect of aquifer heterogeneity on thermal plume dynamics. Since the traditional procedures assuming homogeneous conductivity might lead to an incorrect design or an erroneous interpretation of the plant performance, we shall consider a stochastic approach (Dagan, 1989; Rubin, 2003; Fiori et al., 2015a; Kitanidis, 2015) to evaluate the effect of heterogeneity on shallow geothermal systems. By increasing the conductivity heterogeneity, preferential flow paths emerge, thereby altering the temperature distribution at the production well (Pandey et al., 2018). Moreover, data scarcity does not allow a highly detailed description of the spatial variability of conductivity (Nowak et al., 2010; Maya et al., 2018). Consequently, such a lack of knowledge leads to high uncertainty in the predicted values. More precisely, heterogeneity in hydraulic conductivity could significantly affect the metrics used to evaluate the efficiency of geothermal systems. One of the most considered metrics is the *thermal breakthrough time* (Clyde and Madabhushi, 1983), which is defined as the first arrival time of a thermal plume travelling back to the production well and is ruled by the flow patterns in the well doublet. Another metric is the *recirculating ratio*, which quantifies the fraction of the injected water returning to the production well and it is an indicator of the long-term sustainability of the system (Milnes and Perrochet, 2013).

So far, a small number of studies have investigated the impact of heterogeneity on the geothermal systems. Liu et al. (2019) examined the response of a well pair system in a heterogeneous geothermal reservoir during continuous time operation. They studied how the variability of hydraulic conductivity, heat capacity and correlation length affect the well pair performances. They showed that breakthrough time decreases with increasing heterogeneity degree and correlation length values. Babaei and Nick (2019) addressed low-enthalpy well doublets with an initial temperature of 75°C and a reinjection at 30°C. In particular, they hypothesized a heterogeneous and spatially correlated porosity field (assessing the effect of different values of variance and correlation length) and a permeability field that varies accordingly. They found that an increase of variance and/or correlation length of the porosity (and, hence, permeability) results in a decrease of the well doublet lifetime, defined as the time it takes for the abstracted water temperature to be reduced by 1°C. The same lifetime definition was previously used by Crooijmans et al. (2016) and by Willems et al. (2017) for a sedimentary fluvial reservoir considering different facies realizations. Watanabe et al. (2010), on the other hand, modelled a Hot Dry Rock reservoir with an equivalent porous medium approach, focusing on the propagation of the thermal plume downstream the reinjection well. They found that this phenomenon is mostly influenced by permeability and, to a lesser extent, by the thermal capacity, whereas the thermal conductivity has a negligible influence. The aforementioned studies focused on deep geothermal systems, which are generally characterized by low intrinsic permeabilities (10^{-18}-10^{-12} m^2 according to Moeck (2014)) and large temperature differences between abstraction and reinjection, i.e., in the order of tens of centigrade degrees. Shallow open-loop geothermal systems are installed in more permeable formations (10^{-11}-10^{-9} m^2 according to Sethi and Di Molfetta (2019)) and adopt temperature differences within a few degrees (e.g., ± 4K according to Casasso et al. (2020)). To the authors' knowledge, so far no study has addressed the impact of the heterogeneity of subsurface properties on the operation of shallow open-loop geothermal systems.

The aim of this work is to test the impact of hydraulic conductivity heterogeneity on heat transport in open-loop shallow systems through a stochastic modelling framework. Our objectives are the following:

- Focusing on the interplay between heterogeneity and several thermo-hydro-geological parameters (e.g. thermal diffusion or pore-scale dispersivity) and engineering parameters (e.g., wells arrangement or operational pumping rates).

- Analyzing the behavior of the breakthrough time, i.e. the shortest time a water particle employs to move from the injection to the extraction well, and the recirculating ratio as a function of the main design parameters.
- Comparing the numerical results with the analytical solutions available in literature, in order to test the potentialities and limitations of more simplified approaches.
- Assessing the uncertainty due to the limited knowledge of the subsurface characterization and its effect on the system performance.

The paper is structured as follows. Section 2 presents the methodology by describing the thermal feedback problem, the theoretical framework of heat transport in heterogeneous porous media, and the numerical modelling setup. Section 3 presents the results divided into the analysis of the thermal breakthrough time, the recirculating ratio, the temperature at the pumping well and the ergodicity issue, discussing the main findings and the relationship with existing literature. Conclusions are reported in Section 4.

2. Methodology

2.1. Problem statement

In this work we consider an open-loop shallow geothermal system for the heating of buildings (though the same approach can also be applied to a cooling plant). The geothermal system consists of a well doublet placed into a confined aquifer of constant thickness B. A uniform-in-the-mean regional flow crosses the aquifer. Assuming a system of reference $\mathbf{x} = \{x_1, x_2, x_3\}$, the regional flow is aligned to x_1. Groundwater is abstracted upstream and, after the heat exchange, it is reinjected downstream with a constant lower temperature. The angle between the regional flow and the well doublet is defined as θ and it is measured as shown in Figure 1. The wells in the doublet are placed at a distance L. The two wells are working at a constant rate Q_w, so that the model is steady-state for flow and transient for heat transport.

The pumping activity modifies the natural flow field and determines a local inversion of groundwater flow in the zone between the two wells. If the injected water reaches the extraction well, we have the so called *thermal feedback*, which determines a progressive alteration of the water temperature at the production well T_{prod} with a consequent decrease of the system efficiency. The occurrence of the thermal feedback depends on hydrogeological characteristics, such as the hydraulic conductivity K, the regional-flow gradient $\mathbf{J} = \{J, 0, 0\}$ and the aquifer depth B, as well as engineering parameters, such as the pumping rate Q_w and the wells spatial arrangement (i.e. the well distance L and the angle θ).

This problem can be studied by interpreting heat as a tracer moving in a porous medium. Such an assumption is valid under Local Thermal Equilibrium (LTE) between the rock and the fluid (Shook, 2001; Hoehn and Cirpka, 2006; Markle and Schincariol, 2007; Hecht-Méndez et al., 2010; Stauffer et al., 2019; Irvine et al., 2015; Sarris et al., 2018; Gossler et al., 2019). As a consequence, the thermal plume moves through both pores and soil matrix and thus it is slower than the fluid velocity. The thermal retardation factor R_{th} can be quantified as the ratio between the thermal capacity of the porous medium and the thermal capacity of water, as follows (Shook, 2001):

$$R_{th} = \frac{\rho_s c_s}{n \rho_w c_w} \tag{1}$$

where ρ_w and ρ_s are the water and the solid matrix densities, respectively, c_w and c_s the specific heat capacities of water and solid matrix, respectively, and n is the porosity.

The thermal breakthrough time τ_0, namely the shortest time a water particle spends travelling from the injection well to the production well, is the metric commonly adopted to evaluate the thermal feedback. So far, most of practical studies (Gringarten and Sauty, 1975; Lippmann and Tsang, 1980; Clyde and Madabhushi, 1983; Milnes and Perrochet, 2013; Casasso and Sethi, 2015) have evaluated τ_0 by means of a closed analytical solution that assumes a homogeneous domain, a mean regional flow aligned with the pumping wells (i.e. $\theta = 0$) and advective-only transport. Under such hypotheses the analytical breakthrough time τ_0^{an} can be calculated through the complex potential theory as follows (see, e.g., Strack, 2017; Luo and Kitanidis, 2004):

$$\tau_0^{an} = R_{th} \frac{nL}{KJ} \left[\frac{\chi}{\sqrt{\chi - 1}} \tan^{-1} \left(\frac{1}{\sqrt{\chi - 1}} \right) - 1 \right] \tag{2}$$

where χ is the dimensionless pumping rate

$$\chi = \frac{2Q_w}{\pi BKJL} \tag{3}$$

Providing that the aforementioned assumptions are satisfied, the thermal feedback occurs only when $\chi > 1$ (Luo and Kitanidis, 2004).

In order to evaluate the sustainability of an open-loop system, designers also need to quantify the long-term effect. A typical metric is the fraction of injected water returning to the production well RR, which provides the indication of the efficiency decay of the plant. As well as for τ_0^{an}, a closed form analytical solution can be introduced to assess RR^{an} under the assumption of advective transport and well doublet aligned with the mean flow (Milnes and Perrochet, 2013):

$$RR^{an} = \frac{2}{\pi}\left[\tan^{-1}\left(\sqrt{\chi - 1}\right) - \frac{\sqrt{\chi - 1}}{\chi}\right] \quad (4)$$

We emphasize that these analytical formulae (e.g. eqs. (2) and (4)) are obtained assuming only convective heat transport, neglecting conduction, medium heterogeneity and other pore-scale dispersive/diffusive phenomena. Introducing these more realistic phenomena or angle θ different from zero requires the use of numerical solution schemes. Moreover, these solutions neglect the spreading of the flow trajectories operated by the natural heterogeneity of real aquifers. Heterogeneity determines the emergence of fast flow paths and stagnation zones in the medium, thereby exerting a significant impact on τ_0 (Wen and Gómez-Hernández, 1996; Zinn and Harvey, 2003; Knudby and Carrera, 2006; Fiori and Jankovic, 2012). Given that in the ergodic case τ_0 assumes values in the range $(0, +\infty)$, a significant deviation from the equivalent homogeneous solution is expected in heterogeneous media. In the next sections, we present the mathematical framework and the numerical setup to study open-loop shallow systems in heterogeneous porous media.

2.2. Theoretical framework

Figure 1 depicts a sketch of the conceptual model considered here. We assumed that the flow field occurs in a 3-D confined and stratified aquifer, which is made of N layers, each one characterized by a random homogeneous hydraulic conductivity K_i, for $i = 1, N$. The log-conductivity field $Y = \ln K$ is modeled as a stationary random variable normally distributed with mean $\ln(K_G)$, with K_G the geometric mean of K, and variance σ_Y^2 (Freeze, 1975; Fiori et al., 2015b). The thickness of each layer is $2I_v$, with I_v the vertical integral scale of Y, such that the number of layers is $N = B/(2I_v)$. Water is injected over the total thickness of the aquifer, in such a way that each layer conveys a flux proportional to the local K_i (see, e.g., Kreft and Zuber, 1978; Demmy et al., 1999; Frampton and Cvetkovic, 2009). This stratified-formation conceptual scheme is quite common in groundwater studies dealing with contaminant migration in groundwater (e.g. Zavala-Sanchez et al., 2009; Pedretti and Fiori, 2013; Zech et al., 2018) and can be considered suitable for systems with $L < I_h$, with I_h the Y horizontal integral scale.

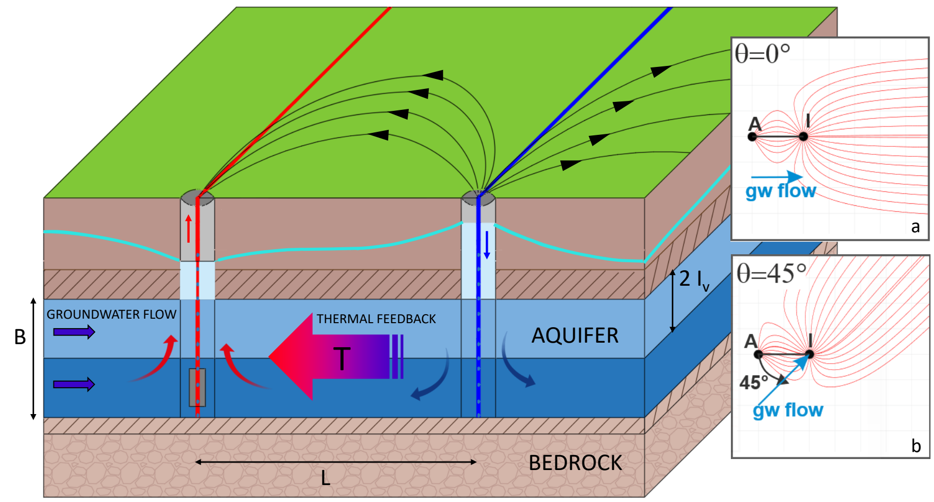

Figure 1: A sketch of the conceptual model. The porous formation is a 3-D confined and stratified aquifer. It is composed of a series of N layers of conductivity K_i, with $i = 1, N$. The conductivity is a stationary random variable lognormaly distributed. A well doublet operating as a geothermal system is placed at the center of the domain. Insets a and b show two configurations of the angle θ between the wells and the regional flow.

At the beginning of the simulation, groundwater is at a constant temperature T_{ref}. After being extracted from the production well, water is reinjected in the injection well at a different temperature T_{well}. As a consequence, a heat plume develops from the injection well, and part of this flow can reach the production well located upstream. Heat transport in geothermal system results from the interplay of different physical phenomena such as conduction, thermal advection and thermal dispersion (Carlslaw and Jaeger, 1959). Conduction is the direct microscopic transfer of kinetic energy between atoms and molecules. It results in heat moving in the opposite direction of temperature gradient. Thermal advection is the transport of heat due to the motion of a fluid moving from one place to another. Thermal dispersion is the heat exchange occurring in porous media due to the nonuniformity in temperature and velocity at the pore-scale

(Özgümüş et al., 2013).

Under LTE, heat transport in porous media can be modelled in a similar way to the transport of solutes. Thus at the Darcy-scale, heat transport can be described by the advection-dispersion equation for solute transport (De Marsily, 1986):

$$-\nabla\left(\frac{\mathbf{q}}{n}T\right)+\nabla\left(D\nabla T\right)+\frac{q_H}{n\rho_w c_w}=R_{th}\frac{\partial T}{\partial t} \tag{5}$$

where T is the local temperature, q_H the heat source, $\mathbf{q}$ the water flux at the Darcy-scale, related to advection, and D is the thermal dispersion which accounts for the heat transfer at pore scale. The thermal dispersion D is given by the sum of two different components, the thermal diffusion D_{th} and the pore-scale dispersion D_α:

$$D=D_{th}+D_\alpha=\frac{\lambda}{n\rho_w c_w}+\alpha_d\frac{|\mathbf{q}|}{n} \tag{6}$$

where λ is the effective thermal conductivity of the medium, α_d the pore-scale dispersivity, here assumed as isotropic, and $|\mathbf{q}|$ is the magnitude of the local velocity. The water flux can be described by the well known Darcy equation:

$$\mathbf{q}=-K\nabla\phi=-K\mathbf{J} \tag{7}$$

where ϕ is the hydraulic head.

Eq. (5) assumes constant water density and viscosity, thus neglecting the temperature dependence on these properties. The limited temperature ranges at which shallow geothermal systems operate (i.e., up to ±6°C compared to background temperature) induce a slight variation of water properties that makes this assumption plausible, as reported in Hecht-Méndez et al. (2010). Under such hypotheses, eq. (5) is formally identical to the *advection dispersion equation*, which describes the solute migration of a sorbing solute in groundwater (Shook, 2001; Hidalgo et al., 2009). By taking advantage of such a mathematical and conceptual equivalence, transport is simulated with a particle tracking procedure developed along a Lagrangian framework. This approach has been extensively used and tested in studies dealing with the solute transport in heterogeneous aquifers with several levels of complexity (Cortis and Berkowitz, 2005; Salamon et al., 2006; Rizzo et al., 2019).

The procedure adopted here is the equivalent random walk formulation of eq. (5), which aims to mimic the water and heat transport in the domain (Kinzelbach, 1988; Uffink, 1988). We consider a water parcel which, once released in the injection well with temperature T_{well}, moves in the flow domain following a flow path. The "total" trajectory $\mathbf{X}(t)$ of the water parcel can be written as the sum of two independent components: i) the advective one related to the Darcy-scale advective velocity, and ii) the fluctuation component $\mathbf{X}'(t)$ which represents phenomena acting at the pore or microscopic scale. The fluctuation, which summarizes the effects of pore-scale dispersion and conduction, is described here by a Wiener process characterized by the local dispersion coefficient $D = D_{th} + D_{\alpha}$ (see eq. (6)). In the following, we shall adopt for simplicity an isotropic pore-scale tensor. The total trajectory $\mathbf{X}(t)$ can be written as:

$$\mathbf{X}(t) = \mathbf{X_0} + \int_0^t \mathbf{v}(\mathbf{x}, t-\tau) d\tau + \mathbf{X}' \tag{8}$$

with $\mathbf{X_0}$ the initial position of the particle and

$$\mathbf{X}' \in N[0, 2Dt/R_{th}] \tag{9}$$

where $\mathbf{v}(\mathbf{x}, t) = \mathbf{q}(\mathbf{x}, t)/(n\, R_{th})$ is the local Darcy-scale advective velocity in the position $\mathbf{x}$ at time t. The dispersion term plays a key role: it determines the deviation of the water particles from the advective streamlines, thereby triggering mixing, macrodispersion and heat dispersion phenomena (Rubin et al., 1999; Shook, 2001; Villermaux, 2012; Le Borgne et al., 2013; Dentz and de Barros, 2015; Di Dato et al., 2018). Given that the heat transport occurs along the flow paths, their ensemble constitutes the heat plume, namely the portion of the domain with temperature affected by the heat injection. Since the temperature is regarded as a tracer associated to the water particles, its assessment in a given position of the flow field would require an ensemble average over different realizations. However T_{prod} at the extraction well can be obtained by taking the average over the flow paths entering in the well and invoking the ergodicity (Dagan, 1991).

In this work we adopt a numerical scheme for the Lagrangian particle tracking procedure. Beside the two lumped parameters τ_0 and RR, we analyze the temperature evolution at the production well. In fact, although the two metrics τ_0 and RR can be used for a fast assessment of the geothermic plant efficiency, they do not give any information on the temperature evolution at the production well, which in turn assesses the plant efficiency evolution in time.

2.3. Numerical setup

On the line of the theoretical framework discussed in the previous section, we developed a numerical code to investigate how spatial heterogeneity, thermal dispersion and engineering parameters affect the thermal feedback metrics, i.e. τ_0 and RR, and the temperature evolution at the production well. The flow field is solved by means of the finite volume scheme of MODFLOW-2005 (Harbaugh, 2005), which is managed through the FloPy python script (Bakker et al., 2016). The thermal propagation is modelled by following the Lagrangian approach through the particle tracking procedure outlined in Di Dato et al. (2019). The injected mass is modelled with a cloud of particles and transport is simulated by tracking them according to the Itô–Taylor integration scheme (Itō, 1951):

$$\mathbf{X}_p(t + \Delta t) = \mathbf{X}_p(t) + \mathbf{A}(\mathbf{X}_p, t)\Delta t + \mathbf{B}(\mathbf{X}_p, t)\, \boldsymbol{\epsilon}\sqrt{\Delta t} \tag{10}$$

where $\mathbf{X}_p$ is the particle position at the initial time t, Δt is the numerical time step, $\boldsymbol{\epsilon}$ is a vector of independent normally distributed random numbers with zero mean and unit variance and the tensors $\mathbf{A}$ and $\mathbf{B}$ are defined, respectively, as (Kinzelbach, 1988; Uffink, 1988):

$$\mathbf{A} = \mathbf{v} + \nabla \cdot \left(\frac{D}{R_{th}} \right) \mathbf{I} \tag{11}$$

$$\mathbf{B} \cdot \mathbf{B}^T = \left(2 \frac{D}{R_{th}} \right) \mathbf{I} \tag{12}$$

where $\mathbf{I}$ is the identity tensor. The time step Δt is chosen by following the particle tracking procedure outlined in Di Dato et al. (2019, see Appendix A). The authors proposed a modified version of the algorithm of Pollock (1988) to model diffusion and pore-scale dispersion. Di Dato et al. (2019) verified the accuracy of their algorithm by comparing the numerical results with a 3^{rd} order Runge-Kutta scheme (Drummond et al., 1984) and the analytical solution of Moench (1989) obtaining a very good match.

As the focus of this paper is on the production of shallow geothermal energy for heating and cooling of buildings, the system domain is chosen to model the typical size of a small installation, e.g. for a detached house, in which the available space for well distancing is not large. The numerical domain depicts a perfectly stratified porous medium with a constant depth $B = 10$ m divided in 10 layers of thickness equal to $2I_v = 1$ m. Such a value of I_v

is consistent with the values encountered in natural porous formations (Rubin, 2003). Each layer is homogeneous and characterized by a random log-conductivity $Y = \ln K$ drawn from a normal distribution with mean $\ln(K_G)$ and variance σ_Y^2. In stratified media the geometric mean is given by $K_G = K_{eff}/\exp(\sigma_Y^2/2)$, where the effective conductivity K_{eff} is equivalent to the arithmetic mean of K. We stress that here the definition of K_{eff} refers to a system subject only to regional flow and it is not a property of strongly nonuniform well flow (Bellin et al., 2020). The dimensionless pumping rate χ in heterogeneous media is therefore defined as:

$$\chi = \frac{2Q_w}{\pi B K_{eff} J L} \tag{13}$$

We explore three heterogeneous scenarios ranging from homogeneous ($\sigma_Y^2 = 0$) to mild heterogeneity degree, i.e. $\sigma_Y^2 = 1$ and 2.

Two fixed heads are assigned to the left and the right boundaries, such that a regional flux develops from left to right. In order to model a confined aquifer, the hydraulic heads are set higher than the aquifer top. Two wells are located at the center of the computational domain at a distance of $L = 10$ m and the line joining the wells forms an angle of θ with the regional flux. As stated in Casasso and Sethi (2015), the convention adopted is that θ is measured counterclockwise from the line joining the wells. The upstream well is extracting and the downstream one is injecting water at equal constant rate Q_w, in such a way to create an open loop. Three setups are considered here: $\theta = 0, \pi/4$ and $\pi/2$. The pumping rate is chosen in such a way to investigate χ ranging from 2 to 12. The 3-D computational grid is $7L \times 7L = 70$ m $\times$ 70 m in the horizontal direction, which suffices to avoid the well influence at the boundaries. The dimensions of the computational cell are $L/50 = 0.2$ m on the horizontal direction and $I_v/4 = 0.125$ m on the vertical direction.

The thermal dispersion is given by the sum of the thermal diffusion D_{th} and pore-scale dispersion D_α, as defined by eq. (6). We consider here four scenarios, given by the combination of $\alpha_d = 0$ and 0.001 m (Fiori and Dagan, 1999) and $D_{th} = 0$ and 10^{-6} m/s^2 (Holman, 2008, Appendix A, Table A-3), which grasp the range of values typically observed in natural aquifers. We highlight that this study focuses on the heterogeneity of the hydraulic conductivity, thereby neglecting the variability of other parameters, such as thermal conductivity and capacity. This choice is justified by the fact that the hydraulic conductivity varies in much wider ranges and has a much stronger influence than both thermal conductivity and capacity. Piga et al. (2017)

highlighted that only the long-term (but not the short-term) propagation of thermal plumes is somehow affected by the thermal conductivity, whereas heat capacity has a negligible effect both in the short and the long term. When it comes to thermal feedback, much shorter time and space scales (i.e. the nearbies of the well doublet) are involved, compared to the propagation of thermal plumes (which develop over larger spatial scales compared to the well doublet distance). For this reason, even thermal conductivity has a secondary effect. Similar conclusions were achieved by Lo Russo et al. (2012).

We modelled the thermal plume by releasing $N_p = 5880$ particles from the injecting well. The injected mass is distributed around the injecting well at every $\pi/60$ radiant and placed uniformly along the depth with an offset of $2I_v$, which is needed in order to avoid boundary effect, from the top and the bottom of the domain. Figure 2 collects a few snapshots of the trajectories resulting from the application of the random walk particle tracking to our numerical system. The plane $x_1 - x_3$ is aligned with the regional flow and $\theta = 0$. The hydraulic conductivity field is generated with variance $\sigma_Y^2 = 2$. The figure shows as the particles placed in the highly-conductive layers travel faster (see dark orange layer in Figure 2). On the contrary, the particles in the low-conductive layers move very slowly (see light yellow layers in Figure 2).

Finally, flow and transport are performed on $MC = 500$ Monte Carlo realizations, which allow to obtain reliable estimates of the ensemble Breakthrough Curve (BTC). For each realization i, we collected the breakthrough time $\tau_{0,i}$ as the time needed for the fastest particle to reach the pumping well, and the recirculating ratio RR_i as the ratio between the number of particles at the pumping well to the total particles. The ensemble breakthrough time $\langle \tau_0 \rangle$ and recirculating ratio $\langle RR \rangle$ are then calculated as

$$\langle \tau_0 \rangle = MC^{-1} \sum_{i=1}^{MC} \tau_{0,i} \tag{14}$$

$$\langle RR \rangle = MC^{-1} \sum_{i=1}^{MC} RR_i \tag{15}$$

Assuming ergodic transport, the breakthrough curve at the pumping well is calculated as the Cumulative Distribution Function (CDF) of the travel times to the well considering all simulations together. The BTC is subsequently scaled with the initial local velocity in order to consider flux-proportional injection (see, e.g., Janković and Fiori, 2010; Pedretti and Fiori, 2013; Fiori et al., 2017; Di Dato et al., 2017). The temperature at the production well is finally

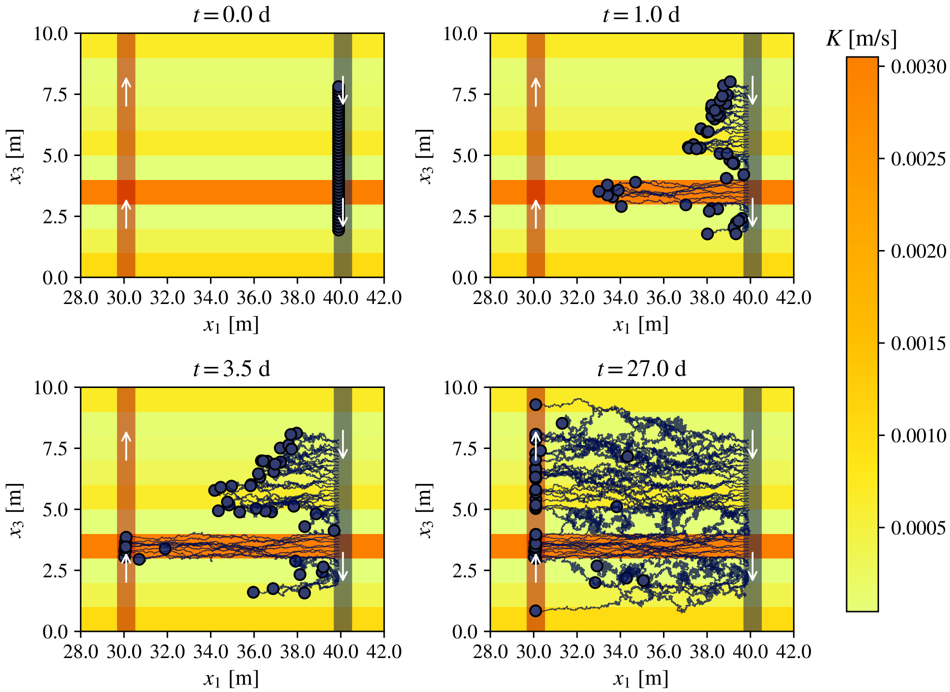

Figure 2: Four snapshots depicting the particle trajectories as a function of time. The plane $x_1 - x_3$ is placed at $x_2 = 0$. The two wells are aligned with the regional flow (i.e. $\theta = 0$). The thermal plume travels in a stratified medium with variance $\sigma_Y^2 = 2$, thermal diffusion $D_{th} = 10^{-6}\text{m/s}^2$ and thermal dispersivity $\alpha_d = 0.001$ m.

calculated by counting the number of particles converging at the production well, as follows (Ferguson, 2006):

$$T_{prod}(t) = \frac{n(t)T_{well} + [N_p - n(t)]T_{ref}}{N_p} \tag{16}$$

where $n(t)$ is the number of particles that have been collected at the time t. The numerical code has been tested in order to verify that the number of Monte Carlo simulations and the number of injected particles are enough to reach statistical convergence.

The parameters used for the simulations and listed in Table 1 were chosen as representative of the geothermal systems typically designed (Galgaro and Cultrera, 2013; Piga et al., 2017). The scenarios comprise two values of hydraulic gradient J, two values for the effective conductivity K_{eff}, three values of angle θ, three values of heterogeneity degree σ_Y^2, two values of α_d and D_{th} and thirteen pumping rates Q_w, for a total of 936 different combinations. In order to keep this number small, we fixed those parameters that impact only the temporal scale at which thermal feedback occurs, such as the porosity n, the aquifer depth B, the distance between the wells L, the thermal retardation factor R_{th} and the temperature difference between the two wells. Generally the introduction of additional variability in the parameters involves an increase of heterogeneity in the results. The findings obtained here could be enhanced by considering, for instance, an heterogeneous porosity or a heterogeneous thermal dispersivity.

Parameter	Description	Value
Fixed parameters		
n	Porosity	0.1
B	Aquifer depth	10 m
L	Distance between the wells	10 m
R_{th}	Thermal retardation factor	3.4 [a]
I_v	Vertical integral scale	0.5 m [b]
T_{well}	Temperature at the injecting well	5°C
T_{ref}	Temperature in groundwater	15°C
Scenarios parameters		
θ	Angle between wells and regional flow	0, $\pi/4$, $\pi/2$
α_d	Pore-scale dispersivity	0, 0.001 m [c]
D_{th}	Thermal diffusion	0, 1e-6 m/s^2 [d]
K_{eff}	Effective conductivity	0.001, 1e-5 m/s [b]
σ_Y^2	Variance of the log-conductivity field	Homog., 1, 2 [b]
J	Hydraulic gradient	0.01, 0.001
Q_w	Pumping rate	$X = [2 - 12]$ [e]

[a] See Casasso and Sethi (2015); [b] See Rubin (2003, Table 2.2); [c] See Fiori and Dagan (1999); [d] See Holman (2008, Appendix A, Table A-3); [e] The pumping rate is set up in order to obtain a χ varying between 2 and 12

Table 1: Model parameters for the numerical experiments.

3. Results and Discussion

Results are shown in terms of breakthrough time τ_0, recirculating ratio RR and temperature at the pumping well T_{prod} for different scenarios. We will analyze separately the impact of pore-scale processes and the angle between the wells and the regional flow. In the first case, the geothermal system is aligned with the groundwater flow (i.e. $\theta = 0$). In the latter case the analysis is carried under pure advection (i.e. $\alpha_d = 0$ and $D_{th} = 0$).

3.1. Breakthrough time

The first analysis we introduce deals with the homogeneous domain. Figure 3 shows the ratio τ_0/τ_{reg} as a function of χ, which represents the dimensionless pumping rate. Results are normalized by $\tau_{reg} = KJ/(R_{th}nL)$, i.e. the time needed to travel the distance L when only regional flow is considered.

In Figure 3a different markers pertain to different couples of (K, J), which determine different flow velocities in the system, whereas different colors are associated to different values of the pore-scale processes α_d and D_{th}. Results show that generally τ_0/τ_{reg} decreases with an exponential behaviour with χ, namely the higher the pumping rate, the shorter the first travel time. Such a result is consistent with previous studies (Milnes and Perrochet, 2013; Casasso and Sethi, 2015). Despite the general behaviour is similar, significant deviations from the purely advective solution can be noticed in the cases with lower velocities. In fact, when advective velocity decreases, the relative importance of diffusion increases. In such a case, the impact of thermal diffusion is not negligible, while the effect of pore-scale dispersivity appears to be always irrelevant in any simulated scenario. The previous analysis is supported by Figure 3b, which depicts a snapshot of the particle trajectories for the considered scenarios with $D_{th} = 10^{-6}$ m/s^2. We highlight that $D_{th} = 10^{-6}$ m/s^2 is the typical thermal diffusion among the values encountered in natural aquifers (Holman, 2008). Inspection of figure shows that when the flow velocity is smaller (scenarios 3 and 4), the dispersion processes prevail and the trajectories assume a more chaotic pattern with respect to the scenarios where the advection prevails (1 and 2). As a consequence, analytical solutions for the geothermal system design should be carefully taken into account even for homogeneous media. In fact, by considering only advection, the analytical eq. (2) might lead to a significant overestimation of the breakthrough time.

The application range of solution τ_0^{an} is explored in Figure 4, where the relative difference in

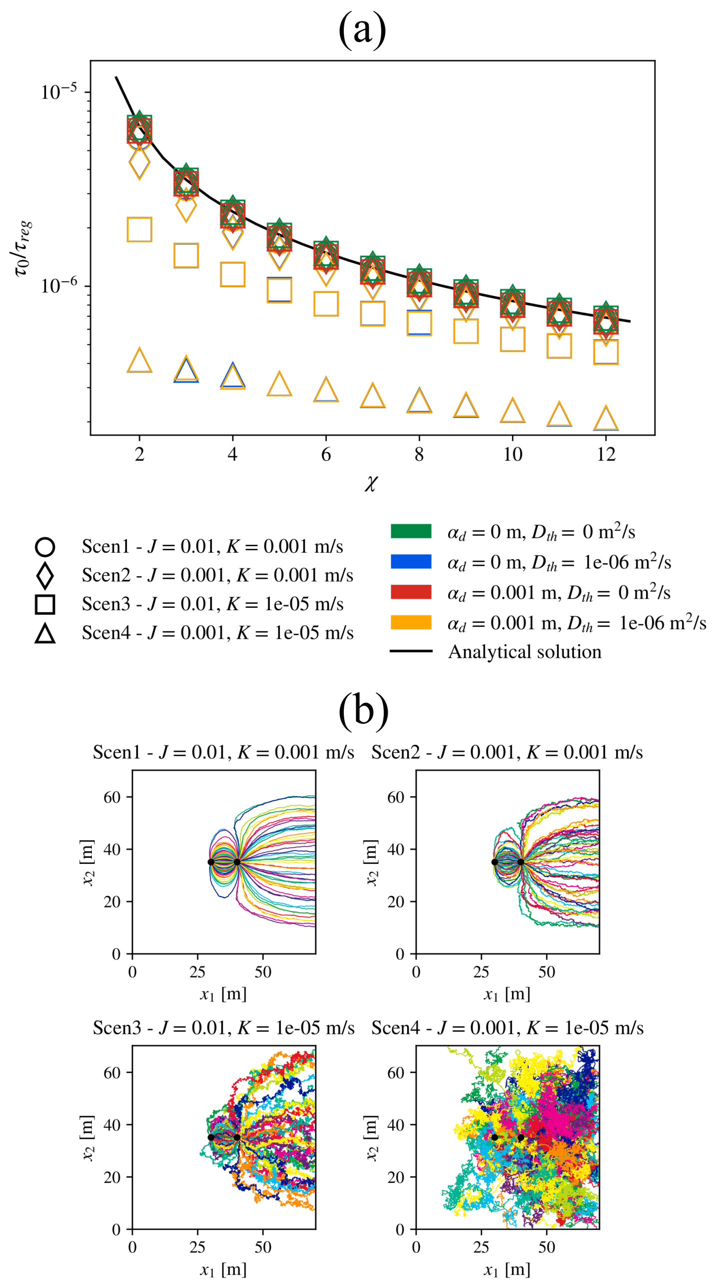

Figure 3: a) Normalized thermal breakthrough times τ_0/τ_{reg} as a function of the dimensionless pumping rate χ for several scenarios depicting different regional flow, i.e. combinations of K and J in a homogeneous medium. Results are normalized by the time a particle needs to cover the distance L under uniform flow and advective transport. b) Pathlines in homogeneous porous media as a result of different combinations of average gradient (J) and hydraulic conductivity values (K) of the porous medium when thermal diffusion is $D_{th} = 10^{-6}$ m/s^2.

predicted breakthrough time $|\tau_0 - \tau_0^{an}|/\tau_0^{an}$ is represented as function of D_{th} and χ. This ratio, namely the normalized absolute error of the analytical solution, approaches the zero value when advection is dominant, while on the opposite case, i.e. when it approaches the value of one, pore-scale heat transport mechanisms play the key role. Scenarios 1 and 2 are characterized by higher flow velocities and are associated with small errors, therefore the analytical solution can be used and the effect of dispersion is negligible. Focusing on the fourth scenario, it is possible to observe how the accuracy of the travel time assessed with eq. (2) decreases with decreasing χ, when the pumping rate is lower. In short, figure 4 confirms that the impact of heat conduction on the breakthrough time is relevant only for low velocity systems, while advective transport prevails in most cases.

We discuss now the effect of the heterogeneity of the hydraulic conductivity K on the breakthrough time τ_0. The medium heterogeneity, defined by the variance of the log-conductivity σ_Y^2, has been recognized as a key parameter in transport problem in natural aquifers, since velocity gradients due to K variability triggers macrodispersion phenomena (Matheron and De Marsily, 1980; Dagan, 1986; De Barros and Rubin, 2011; Zech et al., 2015; Di Dato et al., 2016). In this study we consider two heterogeneity scenarios, depicted by formation with mild heterogeneity degrees, i.e. $\sigma_Y^2 = 1$ and 2. Results are shown as a function of the dimensionless pumping rate χ, which is defined by eq. (13) for the heterogeneous medium. The other parameters governing the regional flow are kept constant and pertain to the second scenario in the previous paragraph, i.e. $J = 0.001$ and $K_{eff} = 0.001$ m/s. It is worth noticing that in stratified media the effective hydraulic conductivity corresponds to the arithmetic mean of K.

As in the previous paragraph, we analyze the mean breakthrough time $\langle\tau_0\rangle$, defined as the expected value of the sample of the breakthrough times. The sample is composed of a number of Monte Carlo simulations, i.e. $MC = 500$. The mean breakthrough time $\langle\tau_0\rangle$ is depicted as a function of χ for four combinations of pore-scale dispersivity α_d and thermal diffusion D_{th}, as shown in Figure 5. The homogeneous solutions and the analytical function (see eq. (14)) are depicted too as reference. Generally the behaviour appears to be similar to the previous analysis, with $\langle\tau_0\rangle$ that decreases for increasing χ values. As expected, the effect of the medium heterogeneity is to reduce the $\langle\tau_0\rangle$, which decreases moving from the homogeneous case to the $\sigma_Y^2 = 1$ and $\sigma_Y^2 = 2$ cases. Such behavior is a consequence of the larger sampling of the higher values of the hydraulic conductivity involved by the higher σ_Y^2. The higher values of K are

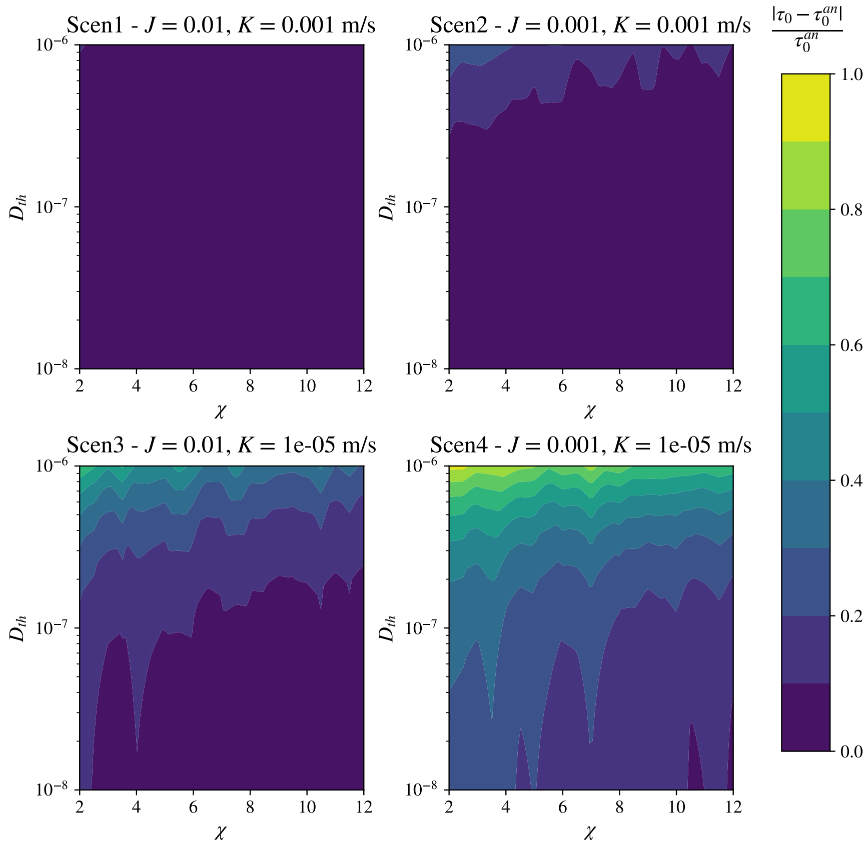

Figure 4: Contour plot of the difference between the numerical τ_0 and the analytical τ_0^{an} (eq. (2)) for χ and D_m and several regional flow scenarios. The plot provides also an indication of the governing transport mechanism, which is advective when $|\tau_0 - \tau_0^{an}|/\tau_0^{an}$ tends to zero and dispersive when $|\tau_0 - \tau_0^{an}|/\tau_0^{an}$ increases.

representative of the fast flow channels which develop in heterogeneous natural formations. As showed in Figure 2, the particles placed in the higher-conductivity layer travel much faster than the other ones. The inset of Figure 5 depicts also the coefficient of variation CV of τ_0 with respect to the MC realizations as a function of χ for several heterogeneity values. For the case $\sigma_Y^2 = 2$, CV shows values higher than 2. This result is of paramount importance because it indicates that τ_0 cannot be considered as a comprehensive index without the assessment of its variability.

When analyzing different geometrical configurations obtained by varying the angle θ between

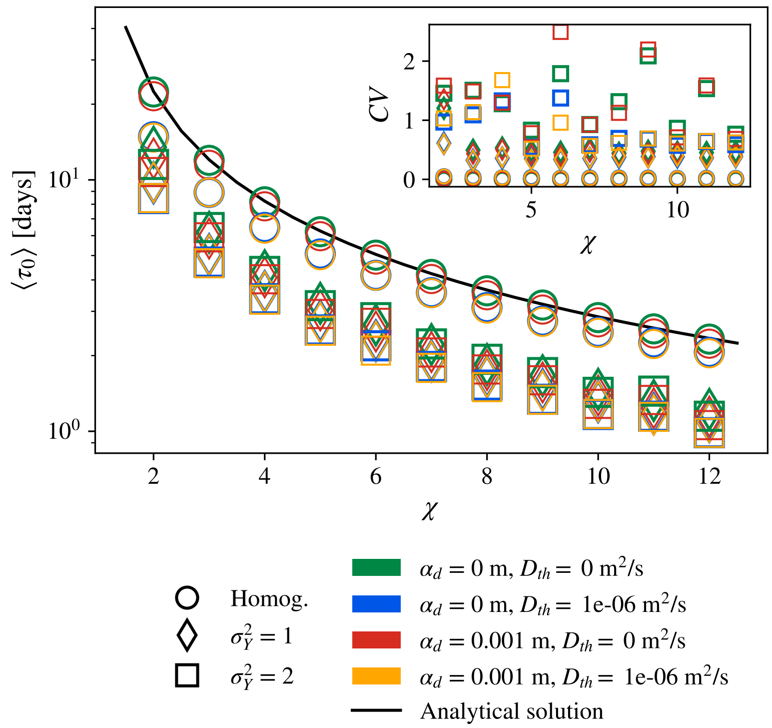

Figure 5: Mean breakthrough time $\langle\tau_0\rangle$ [d] as a function of χ for several values of hydrodynamic dispersion α_d and thermal diffusion D_{th}. The inset depicts the coefficient of variation CV. The mean value and the CV are calculated over a sample of $MC = 500$ Monte Carlo simulations. Results are calculated for a well doublet aligned to the regional flow (i.e. $\theta = 0$).

the wells and the regional flow, the most efficient setup is for θ equal to zero. Otherwise, by increasing the angle between the wells and the regional flow, the breakthrough time decreases, as shown in Figure 6. This result is consistent with previous studies (Milnes and Perrochet, 2013; Casasso and Sethi, 2015). Such an aspect should be taken into consideration in practical application, given that groundwater direction might be affected by seasonal variation (Bellin et al., 1996).

It should be highlighted that in both cases, the results show slight differences in the mean $\langle\tau_0\rangle$ when σ_Y^2 changes from 1 to 2. Liu et al. (2019) performed a similar analysis by studying the relationship between thermal breakthrough time and conductivity heterogeneity with a variance ranging between 0 and 6. As in the present work, they observed that the breakthrough time decreases non-linearly with σ_Y^2, with smaller differences in the higher heterogeneity cases. In contrast, the uncertainty associated to τ_0 in a single realization increases dramatically with

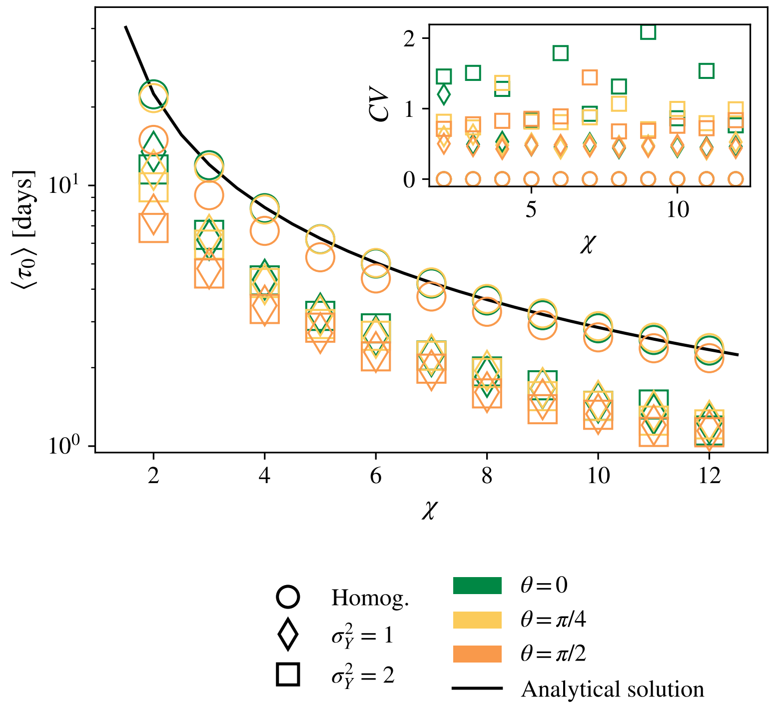

Figure 6: Mean breakthrough time $\langle\tau_0\rangle$ [d] as a function of χ for several values of the angle between regional flow and wells θ. The inset depicts the coefficient of variation CV. The mean value and the CV are calculated over a sample of $MC = 500$ Monte Carlo simulations. Results are calculated under advection-only transport (i.e. $\alpha_d = D_{th} = 0$).

heterogeneity, as shown by the coefficient of variation CV in the insets of both Figures 5 and 6. However, such an uncertainty decreases with the number of layers when ergodicity is reached. Such an issue will be discussed later in a dedicated paragraph.

3.2. Recirculating ratio RR

Along with the breakthrough time, which is an indicator of the early arrivals, the other main operational metric of open-loop geothermal well doublets is the recirculating ratio RR, i.e. the fraction of the flow returning from the injection well to the production well, which is instead an indicator of the long-term effects of returning flow. Figure 7 depicts the effect of pore-scale dispersivity and thermal dispersion for both homogeneous and heterogeneous media on the mean recirculating flow $\langle RR\rangle$. The results show that conductivity heterogeneity as well as thermal dispersion processes generally have a small impact on $\langle RR\rangle$, significant differences can be noticed only for the lower normalized pumping rate $\chi < 6$. Low pumping rate magnifies the effect of preferential paths, thereby increasing the probability of particles to come back to the production well. The coefficient of variation of $\langle RR \rangle$, shown in the inset, increases with σ_Y^2 and decreases with χ pointing at an higher uncertainty in domains characterized by an high heterogeneity degree and a lower pumping rate.

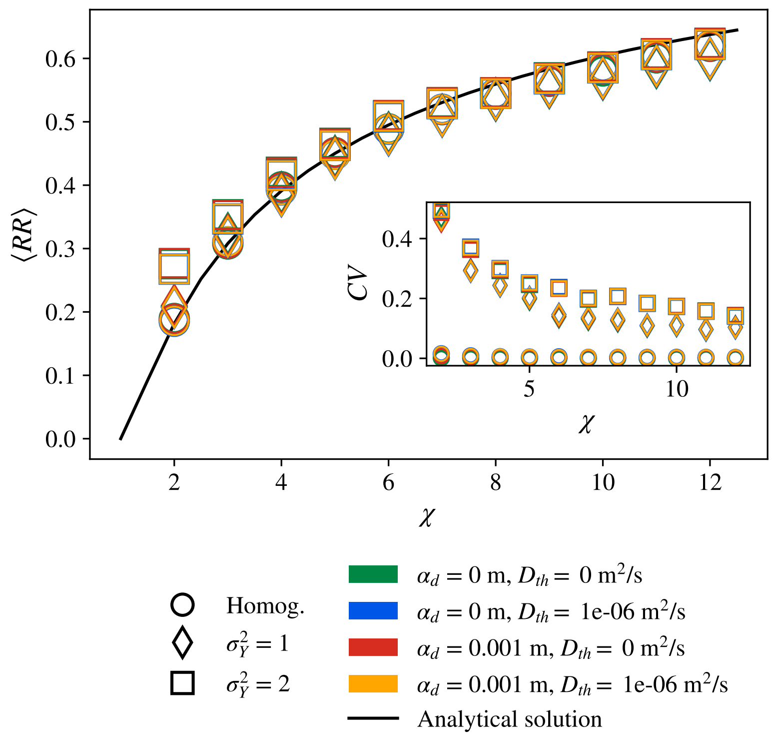

Figure 7: Mean recirculating ratio $\langle RR \rangle$ as a function of χ for several values of hydrodynamic dispersion α_d and thermal diffusion D_{th}. The inset depicts the coefficient of variation CV. The mean value and the CV are calculated over a sample of $MC = 500$ Monte Carlo simulations. Results are calculated for a well doublet aligned to the regional flow (i.e. $\theta = 0$).

Figure 8 shows the mean recirculating ratio $\langle RR \rangle$ as a function of χ for several values of θ, for both homogeneous and heterogeneous media under only advection (i.e. $\alpha_d = D_{th} = 0$). The most efficient configuration is when the wells and the regional flow are aligned, following the breakthrough time behaviour. As in the previous analysis, when χ is large the effect of the heterogeneity is negligible on both the average value of $\langle RR \rangle$ and its variation coefficient.

Furthermore we notice that while the CV for the τ_0 was around one, the CV for RR is smaller than 0.2 for large χ. Such a result indicates that the uncertainty related to the recirculating volume is less affected by heterogeneity than breakthrough time. From a practical point of

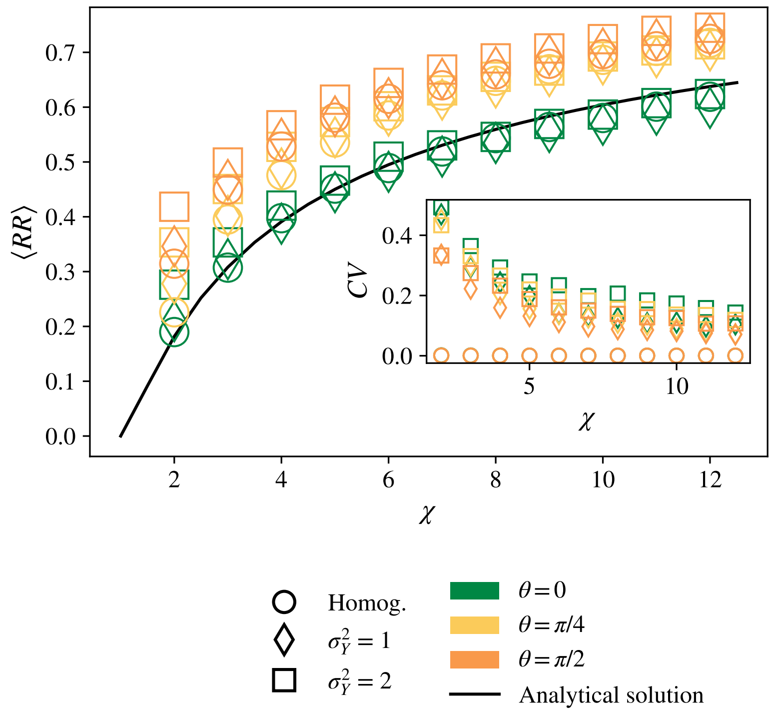

Figure 8: Mean recirculating ratio $\langle RR \rangle$ as a function of χ for several values of the angle between regional flow and wells θ. The inset depicts the coefficient of variation CV. The mean value and the CV are calculated over a sample of $MC = 500$ Monte Carlo simulations. Results are calculated under advection-only transport (i.e. $\alpha_d = D_{th} = 0$).

view, this implies that the recirculating flow rate can be determined by considering the effective conductivity instead of homogeneous conductivity. Consequently, the results from the analytical solution can be a robust evaluation tool.

3.3. Temperature at the pumping well

Evaluating breakthrough times is key to assess whether thermal feedback will occur. Indeed, even if $\chi > 1$, the breakthrough time is often larger than the duration of the heating/cooling season and, hence, the water temperature at the production well remains unaltered. However, the efficiency of the system does not depend on whether thermal breakthrough time occurs or not, but on the time trend of operating temperatures. This holds true *a fortiori* for heterogeneous aquifers, where thermal breakthrough time may occur within a very short time. As depicted by the snapshots in Figure 2, the heterogeneous field is composed of alternating layers of high and low conductivity. Consequently, particles in the high-conductive layers reach the production well earlier than particles in the other zones. In contrast, the particles trapped in the low-conductivity zones extend the arrival time of the last part of the plume. Therefore considering τ_0 only would mislead the evaluation of the operational sustainability of the system. For this reason, we also analyzed the long-term evolution of water temperatures at the production well.

Figure 9 shows the temperature time trends for several typical values of χ and for four combinations of hydrodynamic dispersion α_d and thermal diffusion D_{th}. Figure 10 depicts the temperature evolution as a function of heterogeneity for several values of θ.

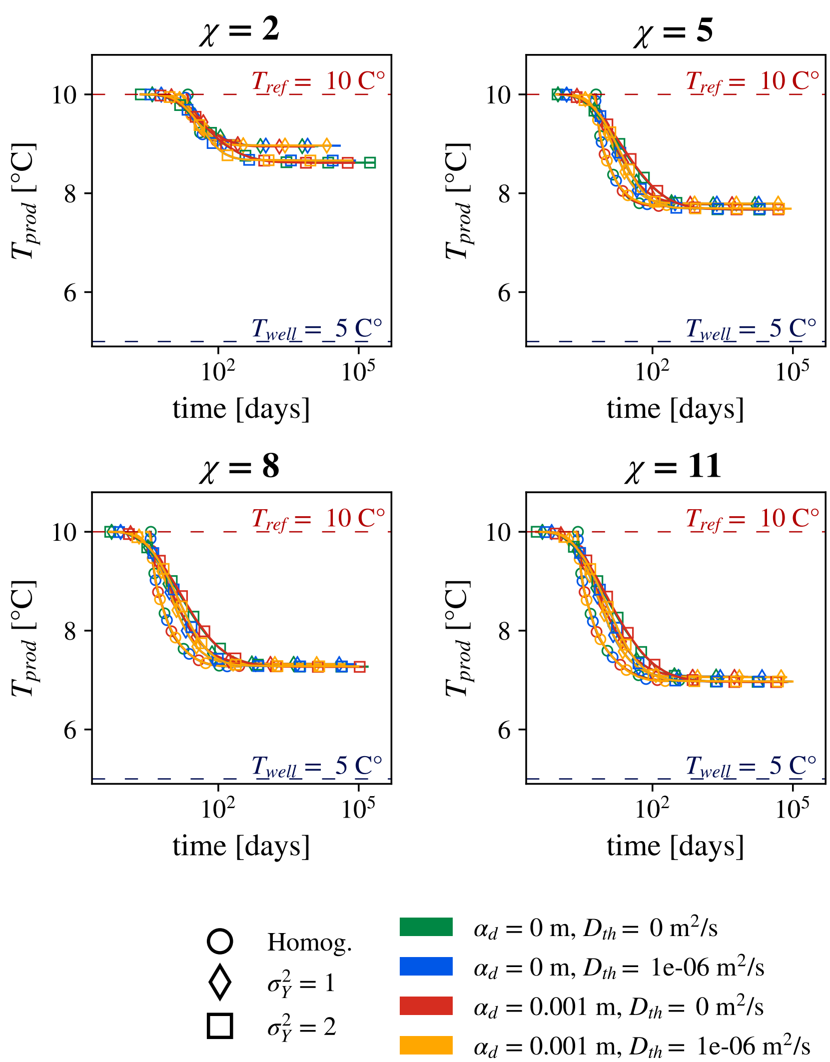

Figure 9: Temperature at the pumping well for several χ values and for four combinations of hydrodynamic dispersion α_d and thermal diffusion D_{th}. Results are calculated for a well doublet aligned to the regional flow (i.e. $\theta = 0$).

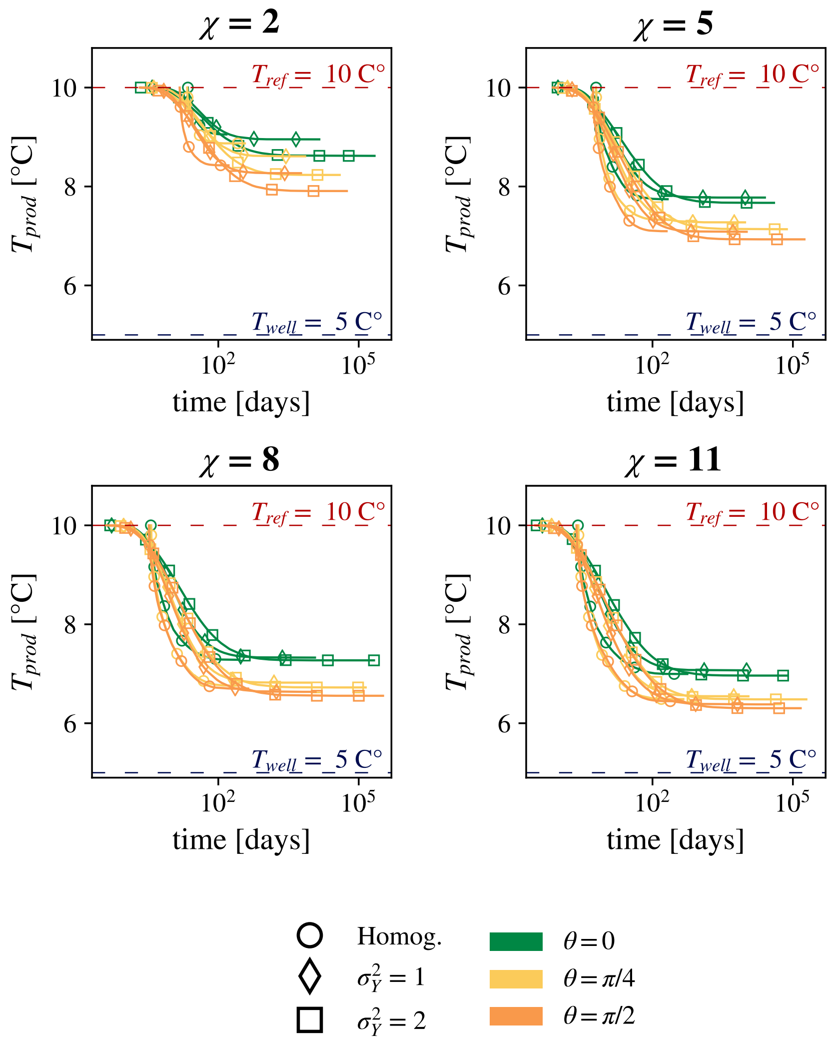

Figure 10: Temperature at the pumping well for several χ values and for several values of θ. Results are calculated under advection-only transport (i.e. $\alpha_d = D_{th} = 0$).

Both figures confirm that the plume dispersion at the production well increases with heterogeneity, in line with experimental evidences (Sauty et al., 1982; Park et al., 2018). Heterogeneity has a strong influence on the breakthrough time and on the shape of thermal breakthrough curve. Also Babaei and Nick (2019) observed a similar behavior. Their study shows that conductivity heterogeneity reduces the time needed to drop the temperature by 1°C when the initial temperature is of 75°C and the reinjection is at 30°C.

In contrast, conductivity heterogeneity is negligible for the long-term development of thermal feedback, as already observed for the recirculating ratio RR. Such behavior becomes more evident by increasing χ, when advection dominates over heat conduction. Although the breakthrough time decreases with heterogeneity, the overall efficiency of the system benefits from it. In fact, the temperature decreases faster when the medium is homogeneous, as shown by the lines with circle markers in Figures 9 and 10. The effect of thermal dispersion on BTC shape increases with medium heterogeneity: while the four BTCs overlap for homogeneous medium, heterogeneity causes a departure in BTCs depending on the D_{th} value. Thermal diffusion accelerates the development of thermal feedback as well, as shown in Figure 9.

The angle θ has a small impact on the thermal breakthrough time, for which the effect of heterogeneity predominates. In contrast, the BTC long-term behavior is controlled mainly by the well doublet angle θ and heterogeneity plays a negligible effect.

3.4. The ergodicity issue

As stated previously, the CV in the insets of Figures 5-8 shows the uncertainty associated to heterogeneity. In the present study, the coefficient of variation indicates the dispersion of the single realizations around their ensemble mean. Here we have considered a sample of $MC =$ 500 Monte Carlo realizations. However, the coefficient of variation decreases by increasing the aquifer depth. When the wells are deep enough to totally grasp the variability of conductivity heterogeneity, the single realization approaches the ensemble mean. Only under such a case, it is possible to assume the ergodic condition, which allows to consider the single realization as representative of the ensemble mean (Kitanidis, 1988; Dagan, 1991; Fiori, 1998; Dentz et al., 2000). Given that well screens usually cross a short depth (typically from a few meters to a few tens of meters), ergodicity could not always be assumed, thereby increasing the uncertainty associated with the predicted ergodic BTC. Figure 11 shows the BTCs for each realization and the ensemble BTCs averaged over an increasing number of Monte Carlo simulations (MC).

For the case considered here, i.e. aquifer depth is composed of ten layers, the single BTC realization can significantly differ from its ergodic counterpart. As a practical consequence, a thermal feedback occurring in a heterogeneous medium could significantly differ from the expected theoretical one, which typically assumes ergodicity. Moreover, the uncertainty of the single realization increases with medium heterogeneity. Figure 11 shows that ergodic conditions are reached averaging over 10 to 20 realizations, which correspond to 100-200 layers according to the heterogeneity degree. As a consequence, the analysis associated to this kind of uncertainty should be carefully considered while designing geothermal systems in heterogeneous media.

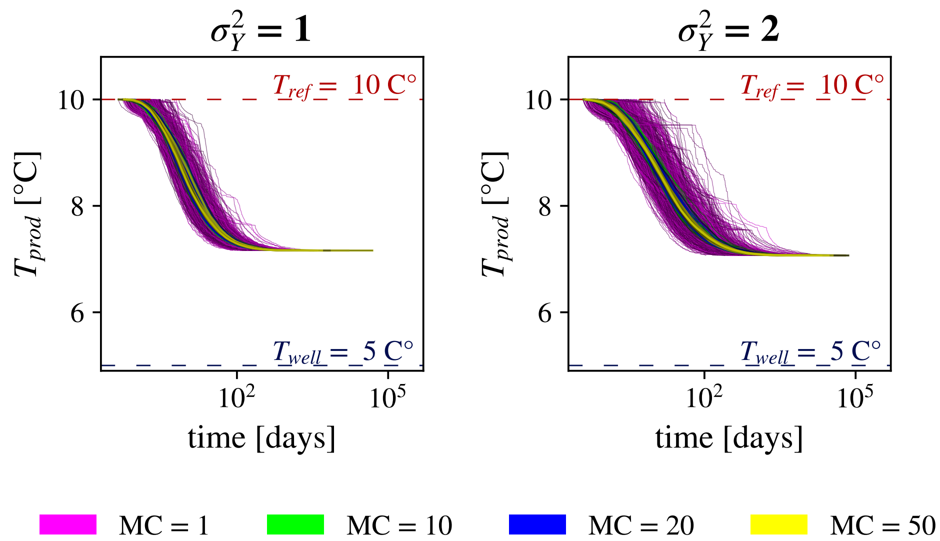

Figure 11: Sample of BTCs used ($MC = 500$ realizations) and the ensemble BTC as function of the MC simulations (layers).

This last issue is of paramount importance in studies dealing with the efficiency of geothermal systems. When the exploitation plant is made of wells crossing a small number of geological formations, the temperature evolution in time can significantly differ with the expected one, based on model results, whose parameters are usually defined by a limited number of tests. In contrast, modeling results are more reliable when the wells cross a large number of geological formations. Finally we highlight that additional sources of uncertainty on results could arise considering variability in other parameters, such as the porosity or the thermal dispersion, which are kept constant within this extensive analysis. Despite this we believe that our results can be considered as general and can provide a suitable basis for a more reliable efficiency assessment of shallow geothermal energy systems.

4. Conclusions

The present study analyzed the interplay of thermal dispersion and macrodispersion in heat transport, thereby focusing on the role of heterogeneity and thermal dispersivity in the design of open-loop shallow geothermal systems. We analyzed the following metrics: the breakthrough time, corresponding to the time the reinjected water needs to reach the production well; the recirculating rate, i.e. the fraction of injecting water returning to the production well; and the temperature curve at the production well.

The main findings are:

- The effects of thermal dispersion parameters are strictly related to the pumping rates and, in general, to the groundwater velocity values. In general, thermal dispersion becomes appreciable in systems characterized by low pumping rates.

- The heterogeneity has a strong impact on the early operational time of geothermal well doublets. Due to channeling, the thermal plume travels faster in the highly conductive layers. As a result, the breakthrough time decreases with heterogeneity. Moreover, the uncertainty associated with early arrivals increases with heterogeneity. Such behavior confirms evidences already observed by Liu et al. (2019) and Babaei and Nick (2019).

- The heterogeneity, as well as dispersion and convection, has a negligible effect on the long-term period. The recirculating ratio depends strongly on the parameter χ and the angle θ, namely it can be modelled by assuming advection only. Therefore the analytical solution for the recirculating ratio RR^{an} gives a robust assessment of the long-term system sustainability.

- The thermal plume spreads more when increasing the variance of medium conductivity. The breakthrough time can therefore be misleading as an indicator of the system efficiency and the whole thermal BTC should be considered. Heterogeneity should be carefully considered, because trajectory dispersion magnifies the variance of arrival times. In highly heterogeneous aquifers, the time span between thermal breakthrough time and a substantial development of thermal feedback can be long enough for the heating/cooling season to end. Consequently the system could benefit from the medium heterogeneity. On the other hand, the uncertainty due to non-ergodic conditions should be taken into serious consideration as well.

The present work can be considered as a first step towards a better understanding of the coupled effect of aquifer heterogeneity and engineering design on the efficiency of shallow geothermal systems. Despite significant assumptions were adopted (i.e. stratified formation, steady state flow, constant injection temperature), the study highlighted and explained noteworthy modelling issues. For instance, we found that heterogeneity has a minor impact on the long-term behavior, but it has a tremendous impact on the short-term counterpart. As a consequence, the assessment of the system efficiency should rely not only on the breakthrough time, but also on the complete temperature evolution at the production well. In contrast, simplified analytical solutions assuming only advection work well to assess the long-term sustainability of the system.

Acknowledgements

The authors gratefully acknowledge the valuable contribution of Sofia Credaro, who assisted in the proofreading and language editing of the manuscript.

References

Babaei, M., Nick, H.M., 2019. Performance of low-enthalpy geothermal systems: interplay of spatially correlated heterogeneity and well-doublet spacings. Applied Energy 253, 113569. doi:10.1016/j.apenergy.2019.113569.

Bakker, M., Post, V., Langevin, C.D., Hughes, J.D., White, J.T., Starn, J.J., Fienen, M.N., 2016. Scripting modflow model development using python and flopy. Groundwater 54, 733–739. doi:10.1111/gwat.12413.

Banks, D., 2009. Thermogeological assessment of open-loop well-doublet schemes: a review and synthesis of analytical approaches. Hydrogeology Journal 17, 1149–1155. doi:10.1007/s10040-008-0427-6.

Banks, D., 2012. An introduction to thermogeology: ground source heating and cooling. John Wiley & Sons.

Barla, M., Di Donna, A., Baralis, M., 2018. City-scale analysis of subsoil thermal conditions due to geothermal exploitation. Environmental Geotechnics 7, 306–316. doi:10.1680/jenge.17.00087.

Bartolini, N., Casasso, A., Bianco, C., Sethi, R., 2020. Environmental and economic impact of the antifreeze agents in geothermal heat exchangers. Energies 13, 5653. doi:10.3390/en13215653.

Bayer, P., Attard, G., Blum, P., Menberg, K., 2019. The geothermal potential of cities. Renewable and Sustainable Energy Reviews 106, 17–30. doi:10.1016/j.rser.2019.02.019.

Bellin, A., Dagan, G., Rubin, Y., 1996. The impact of head gradient transients on transport in heterogeneous formations: Application to the borden site. Water Resources Research 32, 2705–2713. doi:10.1029/96WR01629.

Bellin, A., Fiori, A., Dagan, G., 2020. Equivalent and effective conductivities of heterogeneous aquifers for steady source flow, with illustration for hydraulic tomography. Advances in Water Resources 142, 103632. doi:10.1016/j.advwatres.2020.103632.

Carlslaw, H., Jaeger, J., 1959. Conduction of heat in solids, oxford .

Casasso, A., Sethi, R., 2015. Modelling thermal recycling occurring in groundwater heat pumps (gwhps). Renewable Energy 77, 86–93. doi:10.1016/j.renene.2014.12.003.

Casasso, A., Sethi, R., 2019. Assessment and minimization of potential environmental impacts of ground source heat pump (gshp) systems. Water 11, 1573. doi:10.3390/w11081573.

Casasso, A., Tosco, T., Bianco, C., Bucci, A., Sethi, R., 2020. How can we make pump and treat systems more energetically sustainable? Water 12, 67. doi:10.3390/w12010067.

Clyde, C.G., Madabhushi, G.V., 1983. Spacing of wells for heat pumps. Journal of Water Resources Planning and Management 109, 203–212. doi:10.1061/(ASCE)0733-9496(1983)109:3(203).

Cortis, A., Berkowitz, B., 2005. Computing "anomalous" contaminant transport in porous media: The ctrw matlab toolbox. Groundwater 43, 947–950. doi:10.1111/j.1745-6584.2005.00045.x.

Crooijmans, R.A., Willems, C.J.L., Nick, H.M., Bruhn, D.F., 2016. The influence of facies heterogeneity on the doublet performance in low-enthalpy geothermal sedimentary reservoirs. Geothermics 64, 209–219. doi:10.1016/j.geothermics.2016.06.004.

Dagan, G., 1986. Statistical theory of groundwater flow and transport: Pore to laboratory, laboratory to formation, and formation to regional scale. Water Resources Research 22, 120S–134S. doi:10.1029/WR022i09Sp0120S.

Dagan, G., 1989. Flow and Transport in Porous Formations. Springer-Verlag GmbH & Co. KG.

Dagan, G., 1991. Dispersion of a passive solute in non-ergodic transport by steady velocity fields in heterogeneous formations. Journal of Fluid Mechanics 233, 197–210. doi:10.1017/S0022112091000459.

De Barros, F.P.J., Rubin, Y., 2011. Modelling of block-scale macrodispersion as a random function. Journal of Fluid Mechanics 676, 514–545. doi:10.1017/jfm.2011.65.

De Marsily, G., 1986. Quantitative hydrogeology. Technical Report. Paris School of Mines, Fontainebleau.

Demmy, G., Berglund, S., Graham, W., 1999. Injection mode implications for solute transport in porous media: Analysis in a stochastic lagrangian framework. Water Resources Research 35, 1965–1973. doi:10.1029/1999WR900027.

Dentz, M., de Barros, F.P.J., 2015. Mixing-scale dependent dispersion for transport in heterogeneous flows. Journal of Fluid Mechanics 777, 178–195. doi:10.1017/jfm.2015.351.

Dentz, M., Kinzelbach, H., Attinger, S., Kinzelbach, W., 2000. Temporal behavior of a solute cloud in a heterogeneous porous medium: 1. point-like injection. Water Resources Research 36, 3591–3604. doi:10.1029/2000WR900162.

Di Dato, M., de Barros, F.P.J., Fiori, A., Bellin, A., 2016. Effects of the hydraulic conductivity microstructure on macrodispersivity. Water Resources Research 52, 6818–6832. doi:10.1002/2016WR019086.

Di Dato, M., de Barros, F.P.J., Fiori, A., Bellin, A., 2018. Improving the efficiency of 3-d hydrogeological mixers: Dilution enhancement via coupled engineering-induced transient flows and spatial heterogeneity. Water Resources Research 54, 2095–2111.

Di Dato, M., Bellin, A., Fiori, A., 2019. Convergent radial transport in three-dimensional heterogeneous aquifers: The impact of the hydraulic conductivity structure. Advances in Water Resources 131, 103381. doi:10.1016/j.advwatres.2019.103381.

Di Dato, M., Fiori, A., de Barros, F.P.J., Bellin, A., 2017. Radial solute transport in highly heterogeneous aquifers: Modeling and experimental comparison. Water Resources Research 53, 5725–5741. doi:10.1002/2016WR020039.

Drummond, I., Duane, S., Horgan, R., 1984. Scalar diffusion in simulated helical turbulence with molecular diffusivity. Journal of Fluid Mechanics 138, 75–91. doi:10.1017/S0022112084000045.

Epting, J., García-Gil, A., Huggenberger, P., Vázquez-Suñe, E., Mueller, M.H., 2017. Development of concepts for the management of thermal resources in urban areas–assessment of transferability from the basel (switzerland) and zaragoza (spain) case studies. Journal of Hydrology 548, 697–715. doi:10.1016/j.jhydrol.2017.03.0570.

Ferguson, G., 2006. Potential use of particle tracking in the analysis of low-temperature geothermal developments. Geothermics 35, 44–58. doi:10.1016/j.geothermics.2005.11.001.

Fiori, A., 1998. On the influence of pore-scale dispersion in nonergodic transport in heterogeneous formations. Transport in Porous Media 30, 57–73. doi:10.1023/A:1006548529015.

Fiori, A., Bellin, A., Cvetkovic, V., de Barros, F.P.J., Dagan, G., 2015a. Stochastic modeling of solute transport in aquifers: From heterogeneity characterization to risk analysis. Water Resources Research 51, 6622–6648. doi:10.1002/2015WR017388.

Fiori, A., Dagan, G., 1999. Concentration fluctuations in transport by groundwater: Comparison between theory and field experiments. Water Resources Research 35, 105–112. doi:10.1029/98WR01862.

Fiori, A., Jankovic, I., 2012. On preferential flow, channeling and connectivity in heterogeneous porous formations. Mathematical Geosciences 44, 133–145. doi:10.1007/s11004-011-9365-2.

Fiori, A., Volpi, E., Zarlenga, A., Bohling, G.C., 2015b. Gaussian or non-gaussian logconductivity distribution at the made site: What is its impact on the breakthrough curve? Journal of Contaminant Hydrology 179, 25–34. doi:10.1016/j.jconhyd.2015.05.004.

Fiori, A., Zarlenga, A., Jankovic, I., Dagan, G., 2017. Solute transport in aquifers: The comeback of the advection dispersion equation and the first order approximation. Advances in Water Resources 110, 349–359. doi:10.1016/j.advwatres.2017.10.025.

Frampton, A., Cvetkovic, V., 2009. Significance of injection modes and heterogeneity on spatial and temporal dispersion of advecting particles in two-dimensional discrete fracture networks. Advances in Water Resources 32, 649–658. doi:10.1016/j.advwatres.2008.07.010.

Freeze, R.A., 1975. A stochastic-conceptual analysis of one-dimensional groundwater flow in nonuniform homogeneous media. Water Resources Research 11, 725–741. doi:10.1029/WR011i005p00725.

Galgaro, A., Cultrera, M., 2013. Thermal short circuit on groundwater heat pump. Applied Thermal Engineering 57, 107–115. doi:10.1016/j.applthermaleng.2013.03.011.

Gossler, M.A., Bayer, P., Zosseder, K., 2019. Experimental investigation of thermal retardation and local thermal non-equilibrium effects on heat transport in highly permeable, porous aquifers. Journal of Hydrology 578, 124097. doi:10.1016/j.jhydrol.2019.124097.

Gringarten, A.C., Sauty, J.P., 1975. A theoretical study of heat extraction from aquifers with uniform regional flow. Journal of Geophysical Research 80, 4956–4962. doi:10.1029/JB080i035p04956.

Harbaugh, A.W., 2005. MODFLOW-2005, the US Geological Survey modular ground-water model: the ground-water flow process. US Department of the Interior, US Geological Survey Reston, VA, USA.

Hecht-Méndez, J., Molina-Giraldo, N., Blum, P., Bayer, P., 2010. Evaluating mt3dms for heat transport simulation of closed geothermal systems. Groundwater 48, 741–756. doi:10.1111/j.1745-6584.2010.00678.x.

Hidalgo, J.J., Carrera, J., Dentz, M., 2009. Steady state heat transport in 3d heterogeneous porous media. Advances in Water Resources 32, 1206–1212. doi:10.1016/j.advwatres.2009.04.003.

Hoehn, E., Cirpka, O., 2006. Assessing hyporheic zone dynamics in two alluvial flood plains of the southern alps using water temperature and tracers. Hydrology and Earth System Sciences Discussions 3, 335–364.

Holman, J.P., 2008. Heat Transfer (Si Units) Sie. Tata McGraw-Hill Education.

Horne, R., 1985. Reservoir engineering aspects of reinjection. Geothermics 14, 449–457. doi:10.1016/0375-6505(85)90082-3.

Irvine, D.J., Lautz, L.K., Briggs, M.A., Gordon, R.P., McKenzie, J.M., 2015. Experimental evaluation of the applicability of phase, amplitude, and combined methods to determine water flux and thermal diffusivity from temperature time series using vflux 2. Journal of Hydrology 531, 728–737. doi:10.1016/j.jhydrol.2015.10.054.

Itō, K., 1951. On stochastic differential equations. volume 4. American Mathematical Soc.

Janković, I., Fiori, A., 2010. Analysis of the impact of injection mode in transport through strongly heterogeneous aquifers. Advances in Water Resources 33, 1199–1205. doi:10.1016/j.advwatres.2010.05.006.

Kinzelbach, W., 1988. The random walk method in pollutant transport simulation, in: Groundwater flow and quality modelling. D. Reidel, Norwell, Mass. volume 224, pp. 227–246.

Kitanidis, P.K., 1988. Prediction by the method of moments of transport in a heterogeneous formation. Journal of Hydrology 102, 453–473. doi:10.1016/0022-1694(88)90111-4.

Kitanidis, P.K., 2015. Persistent questions of heterogeneity, uncertainty, and scale in subsurface flow and transport. Water Resources Research 51, 5888–5904. doi:10.1002/2015WR017639.

Knudby, C., Carrera, J., 2006. On the use of apparent hydraulic diffusivity as an indicator of connectivity. Journal of Hydrology 329, 377–389. doi:10.1016/j.jhydrol.2006.02.026.

Kong, Y., Pang, Z., Shao, H., Kolditz, O., 2017. Optimization of well-doublet placement in geothermal reservoirs using numerical simulation and economic analysis. Environmental Earth Sciences 76, 118. doi:10.1007/s12665-017-6404-4.

Kreft, A., Zuber, A., 1978. On the physical meaning of the dispersion equation and its solutions for different initial and boundary conditions. Chemical Engineering Science 33, 1471–1480. doi:10.1016/0009-2509(78)85196-3.

Le Borgne, T., Dentz, M., Villermaux, E., 2013. Stretching, coalescence, and mixing in porous media. Physical Review Letters 110, 204501. doi:10.1103/PhysRevLett.110.204501.

Lippmann, M.J., Tsang, C.F., 1980. Ground water use for cooling: Associated aquifer temperature changes. Ground Water 18. doi:10.1111/j.1745-6584.1980.tb03420.x.

Liu, G., Pu, H., Zhao, Z., Liu, Y., 2019. Coupled thermo-hydro-mechanical modeling on well pairs in heterogeneous porous geothermal reservoirs. Energy 171, 631–653. doi:10.1016/j.energy.2019.01.022.

Lo Russo, S., Taddia, G., Verda, V., 2012. Development of the thermally affected zone (taz) around a groundwater heat pump (gwhp) system: A sensitivity analysis. Geothermics 43, 66–74. doi:10.1016/j.geothermics.2012.02.001.

Lund, J.W., Toth, A.N., 2020. Direct utilization of geothermal energy 2020 worldwide review. Geothermics , 101915doi:10.1016/j.geothermics.2020.101915.

Luo, J., Kitanidis, P.K., 2004. Fluid residence times within a recirculation zone created by an extraction–injection well pair. Journal of Hydrology 295, 149–162. doi:10.1016/j.jhydrol.2004.03.006.

Markle, J.M., Schincariol, R.A., 2007. Thermal plume transport from sand and gravel pits–potential thermal impacts on cool water streams. Journal of Hydrology 338, 174–195. doi:10.1016/j.jhydrol.2007.02.031.

Matheron, G., De Marsily, G., 1980. Is transport in porous media always diffusive? a counterexample. Water Resources Research 16, 901–917. doi:10.1029/WR016i005p00901.

Maya, S.M., García-Gil, A., Schneider, E.G., Moreno, M.M., Epting, J., Vázquez-Suñé, E., Marazuela, M.Á., Sánchez-Navarro, J.Á., 2018. An upscaling procedure for the optimal implementation of open-loop geothermal energy systems into hydrogeological models. Journal of Hydrology 563, 155–166. doi:10.1016/j.jhydrol.2018.05.057.

Milnes, E., Perrochet, P., 2013. Assessing the impact of thermal feedback and recycling in open-loop groundwater heat pump (gwhp) systems: a complementary design tool. Hydrogeology journal 21, 505–514. doi:10.1007/s10040-012-0902-y.

Moeck, I.S., 2014. Catalog of geothermal play types based on geologic controls. Renewable and Sustainable Energy Reviews 37, 867–882. doi:10.1016/j.rser.2014.05.032.

Moench, A.F., 1989. Convergent radial dispersion: A laplace transform solution for aquifer tracer testing. Water Resources Research 25, 439–447. doi:10.1029/WR025i003p00439.

Nowak, W., De Barros, F.P.J., Rubin, Y., 2010. Bayesian geostatistical design: Task-driven optimal site investigation when the geostatistical model is uncertain. Water Resources Research 46. doi:10.1029/2009WR008312.

Özgümüş, T., Mobedi, M., Özkol, Ü., Nakayama, A., 2013. Thermal dispersion in porous media—a review on the experimental studies for packed beds. Applied Mechanics Reviews 65. doi:10.1115/1.4024351.

Pandey, S., Vishal, V., Chaudhuri, A., 2018. Geothermal reservoir modeling in a coupled thermo-hydro-mechanical-chemical approach: a review. Earth-Science Reviews 185, 1157–1169. doi:10.1016/j.earscirev.2018.09.004.

Park, B.H., Lee, B.H., Lee, K.K., 2018. Experimental investigation of the thermal dispersion coefficient under forced groundwater flow for designing an optimal groundwater heat pump (gwhp) system. Journal of Hydrology 562, 385–396. doi:10.1016/j.jhydrol.2018.05.023.

Pedretti, D., Fiori, A., 2013. Travel time distributions under convergent radial flow in heterogeneous formations: Insight from the analytical solution of a stratified model. Advances in Water Resources 60, 100–109. doi:http://dx.doi.org/10.1016/j.advwatres.2013.07.013.

Piga, B., Casasso, A., Pace, F., Godio, A., Sethi, R., 2017. Thermal impact assessment of groundwater heat pumps (gwhps): Rigorous vs. simplified models. Energies 10, 1385. doi:10.3390/en10091385.

Pollock, D.W., 1988. Semianalytical computation of path lines for finite-difference models. Groundwater 26, 743–750. doi:10.1111/j.1745-6584.1988.tb00425.x.

Pophillat, W., Attard, G., Bayer, P., Hecht-Méndez, J., Blum, P., 2020. Analytical solutions for predicting thermal plumes of groundwater heat pump systems. Renewable Energy 147, 2696–2707. doi:10.1016/j.renene.2018.07.148.

Rizzo, C.B., Nakano, A., de Barros, F.P.J., 2019. Par2: Parallel random walk particle tracking method for solute transport in porous media. Computer Physics Communications 239, 265–271. doi:10.1016/j.cpc.2019.01.013.

Rubin, Y., 2003. Applied Stochastic Hydrogeology. Oxford University Press.

Rubin, Y., Sun, A., Maxwell, R., Bellin, A., 1999. The concept of block-effective macrodispersivity and a unified approach for grid-scale-and plume-scale-dependent transport. Journal of Fluid Mechanics 395, 161–180. doi:10.1017/S0022112099005868.

Salamon, P., Fernàndez-Garcia, D., Gómez-Hernández, J.J., 2006. A review and numerical assessment of the random walk particle tracking method. Journal of Contaminant Hydrology 87, 277–305. doi:10.1016/j.jconhyd.2006.05.005.

Sarris, T.S., Close, M., Abraham, P., 2018. Using solute and heat tracers for aquifer characterization in a strongly heterogeneous alluvial aquifer. Journal of Hydrology 558, 55–71. doi:10.1016/j.jhydrol.2018.01.032.

Sauty, J.P., Gringarten, A.C., Fabris, H., Thiéry, D., Menjoz, A., Landel, P.A., 1982. Sensible energy storage in aquifers: 2. field experiments and comparison with theoretical results. Water Resources Research 18, 253–265. doi:10.1029/WR018i002p00253.

Sethi, R., Di Molfetta, A., 2019. Analytical solutions of the groundwater flow equation, in: Groundwater Engineering. Springer, pp. 33–53.

Shook, G.M., 2001. Predicting thermal breakthrough in heterogeneous media from tracer tests. Geothermics 30, 573–589. doi:10.1016/S0375-6505(01)00015-3.

Stauffer, F., Bayer, P., Blum, P., Giraldo, N.M., Kinzelbach, W., 2019. Thermal use of shallow groundwater. CRC Press.

Strack, O.D., 2017. Analytical groundwater mechanics. Cambridge University Press.

Tissen, C., Menberg, K., Benz, S.A., Bayer, P., Steiner, C., Götzl, G., Blum, P., 2021. Identifying key locations for shallow geothermal use in vienna. Renewable Energy 167, 1–19. doi:10.1016/j.renene.2020.11.024.

Tsagarakis, K.P., Efthymiou, L., Michopoulos, A., Mavragani, A., Anelković, A.S., Antolini, F., Bacic, M., Bajare, D., Baralis, M., Bogusz, W., et al., 2020. A review of the legal framework in shallow geothermal energy in selected european countries: Need for guidelines. Renewable energy 147, 2556–2571. doi:10.1016/j.renene.2018.10.007.

Uffink, G.J.M., 1988. Modeling of solute transport with the random walk method, in: Groundwater flow and quality modelling. Springer. volume 224, pp. 247–265.

Villermaux, E., 2012. Mixing by porous media. Comptes Rendus Mécanique 340, 933–943.

Watanabe, N., Wang, W., McDermott, C.I., Taniguchi, T., Kolditz, O., 2010. Uncertainty analysis of thermo-hydro-mechanical coupled processes in heterogeneous porous media. Computational Mechanics 45, 263–280. doi:10.1007/s00466-009-0445-9.

Wen, X.H., Gómez-Hernández, J.J., 1996. Upscaling hydraulic conductivities in heterogeneous media: An overview. Journal of Hydrology 183, ix–xxxii. doi:10.1016/S0022-1694(96)80030-8.

Willems, C., Nick, H., Goense, T., Bruhn, D., 2017. The impact of reduction of doublet well spacing on the net present value and the life time of fluvial hot sedimentary aquifer doublets. Geothermics 68, 54–66. doi:10.1016/j.geothermics.2017.02.008.

Zavala-Sanchez, V., Dentz, M., Sanchez-Vila, X., 2009. Characterization of mixing and spreading in a bounded stratified medium. Advances in Water Resources 32, 635–648. doi:10.1016/j.advwatres.2008.05.003.

Zech, A., Attinger, S., Cvetkovic, V., Dagan, G., Dietrich, P., Fiori, A., Rubin, Y., Teutsch, G., 2015. Is unique scaling of aquifer macrodispersivity supported by field data? Water Resources Research 51, 7662–7679. doi:10.1002/2015WR017220.

Zech, A., D'Angelo, C., Attinger, S., Fiori, A., 2018. Revisitation of the dipole tracer test for heterogeneous porous formations. Advances in Water Resources 115, 198–206. doi:10.1016/j.advwatres.2018.03.006.

Zinn, B., Harvey, C.F., 2003. When good statistical models of aquifer heterogeneity go bad: A comparison of flow, dispersion, and mass transfer in connected and multivariate gaussian hydraulic conductivity fields. Water Resources Research 39.